Journal of Materials and Environmental Sciences
ISSN : 2028-2508

JMES, 2017 Volume 8, Issue 10, Page 3706-3717

http://www.jmaterenvironsci.com/

Artocarpus odoratissimus (Tarap) core as an adsorbent for the removal of crystal violet dye from aqueous solution

M. K. Dahri[1*], M. R .R. Kooh[1], L. B. L. Lim[1]
1. Chemical Sciences, Faculty of Science, Universiti Brunei Darussalam, Jalan Tungku Link, Gadong, Brunei Darussalam

Received 29 Apr 2016,
Revised 23 Apr 2017,
Accepted 28 Apr 2017

Keywords

- ✓ Water remediation;
- ✓ *Artocarpus*;
- ✓ Crystal violet;
- ✓ Biosorption;
- ✓ Wastewater treatment

M.K. Dahri
kiddri86@hotmail.com
+6738875789

Abstract

Tarap core (TC) was used to investigate its ability as an adsorbent for the removal of crystal violet (CV) dye from aqueous solution. Batch experiment was done to evaluate parameters such as effects of contact time, dosage, dye concentration, temperature, pH and ionic strength on the adsorption of CV onto TC. Langmuir, Freundlich and Tempkin isotherm models were used to investigate the adsorption process and the Langmuir model was found to best fit the experimental data with maximum monolayer adsorption capacity of 217 mg g^{-1}. The optimum conditions for the experiments were 2 h contact time and without any pH adjustment. Thermodynamics study indicated that the adsorption of CV onto TC was feasible and endothermic in nature. From the kinetics study, film diffusion and pseudo 2nd order model might play major roles in the adsorption mechanism.

1. Introduction

One of the important necessities in life is water. However, human activities have long contaminate the water sources around the world since the emergence of industrial and agricultural activities. Thus, it is of utmost importance to save these water sources for the use of mankind and all living things [1].

Dye disposal into water sources is one of the major pollutants produced from industrial activities. Synthetic dyes are used in food, textile, tannery, paper and cosmetic industries. Due to their stable nature, they are resistant to biodegradation which can lead to undesired effects on the flora and fauna of the water bodies. Synthetic dyes can prevent sunlight from penetrating into the water, reducing both photosynthetic activity and oxygen dissolution. Due to their aromatic structures, many dyes are considered carcinogenic and mutagenic [2].

Many methods [3] have been devised in order to treat the dye wastewater and one of those methods is adsorption. Adsorption method is fairly simple where the pollutants are adsorbed onto the adsorbent's surface leaving a clear effluent when the adsorbent is taken out. This method is inexpensive and environmental friendly with an abundance of the adsorbent material. In the past decades, adsorption method was extensively studied using various adsorbents such as fruit peel [4], waterferns [5-7], shell [8] and peat [9-11].

The aim of this study was to use *Artocarpus odoratissimus* core as an adsorbent in order to remove crystal violet (CV) dye from aqeuous solution. Experimental parameters such as effects of dosage, ionic strength, contact time, dye concentration, pH and temperature on the adsorption of CV onto Tarap core (TC) were investigated.

Artocarpus odoratissimus, locally known as Tarap, can be found in the tropical regions of South East Asia. The fruit contains white delicious, aromatic and sweet pulps that are attached to the central core. The seeds which are surrounded by the pulps can also be consumed when boiled or roasted while the core and peel are usually thrown away as wastes. Recent studies on the use of Tarap core in the removal of heavy metals [12] and dye [13] using adsorption approach showed promising results. Therefore, TC was chosen in this study in order to explore its possibility to be used as a low cost adsorbent for the removal of toxic CV dye from aqeuous solution.

CV belongs to one of the most important dye class, the triphenylmethane dyes. CV used in detergents, electronics (circuit boards, batteries, transistors), inks and paper printing, and as biological staining agents, antifungal agents and antiseptic agents. However CV dye is also hazardous with some of the known harmful properties which include acute oral toxicity, genotoxicity, mutagenicity and percutaneous toxicity [14]. Hence, there is a need for it to be removed from dye effluents and therefore, CV was chosen in this study as a model dye.

2. Experimental details

2.1 Samples preparations

Tarap fruits were purchased from the local open market and the core was separated from the fruit. The tarap core (TC) was then washed prior to cutting into small pieces and dried in an oven at 85 °C until a constant mass was obtained. The dried TC was then blended and sieved in order to obtain ~355 µm diameter particles.

2.2 Instrumentations and chemicals

Crystal violet (CV, molecular formula $C_{25}H_{30}N_3Cl$, M_r = 407.98 g mol^{-1}) and potassium nitrate were purchased from Sigma-Aldrich. Nitric acid (AnalaR) and sodium hydroxide (Univar) were used to adjust the solution pH. An appropriate amount of CV solid was dissolved in double distilled water to make the stock solution and a serial dilution was used to obtain other lower dye concentrations. The reagents were used without any further purification and double distilled water was used throughout the experiments.

Gallenkamp Hotbox oven was used to dry TC and the dried adsorbent was then blended using Panasonic MX-J210GN blender. EDT instruments GP 353 ATC pH meter was used to measure the solutions' pH. The mixtures of TC and CV were agitated in clean conical flasks using the Stuart orbital shaker set at 250 rpm. Shimadzu UV-1601PC UV–Visible (UV-Vis) spectrophotometer was used for analysis of the dye content and the wavelength for CV was set to 589 nm. Shimadzu IR Prestige-21 spectrophotometer was used for Fourier transform infrared (FTIR) spectroscopy in order to characterise TC's functional groups at spectral range from 4000 to 400 cm^{-1}. The surface morphology of the TC was obtained by using a Tescan Vega XMU Scanning Electron Microscope. The adsorbent was gold coated using SPI-MODULE™ Sputter Coater before the analysis.

2.3 Experimental procedure

TC (0.04 g) was mixed with a known concentration of CV dye solution (20.0 mL) in a 125 mL conical flask and the mixture was then agitated at room temperature. The experiments were conducted in order to investigate adsorption parameters such as dosage (0.01 – 0.06 g), contact time (0 - 240 min), dye concentration (20 – 500 mg L^{-1}), medium pH (2 - 10), temperature (25 – 65°C) ionic strength (0.1 – 0.8 mol L^{-1} NaCl). The dye content was then analysed using UV-Vis spectrophotometer.

The amount of CV adsorbed by a gram of TC was calculated as q_e (mg g^{-1}) and the equation is shown below:

$$q_e = \frac{(C_0 - C_e)V}{m} \tag{1}$$

where C_0 is the initial adsorbate concentration (mg L^{-1}), C_e is the adsorbate concentration at equilibrium (mg L^{-1}), V is the volume of adsorbate solution used (L), and m is the mass of absorbent used (g).

The percentage removal of adsorbate by TC is represented as follows:

$$\text{Percentage removal} = \frac{(C_0 - C_e) \times 100\%}{C_0} \tag{2}$$

2.4 Determination of TC's point of zero charge (pH$_{pzc}$)

A series of CV solutions (100 mg L^{-1}) was prepared by diluting the stock solution using different amount of 1.0 mol L^{-1} NaCl in order to achieve salt concentration in the range of 0 – 0.8 mol L^{-1}. The pH of the mixture solutions was then altered in the range of 2 – 10 before adding TC (0.04 g) into the dye-salt solution (20.0 mL) and agitated for 24 h. The final pH of each mixture was then measured. The graph of ΔpH (pH$_i$ – pH$_f$) versus pH$_i$ was plotted in order to determine the pH$_{pzc}$ where pH$_i$ and pH$_f$ are the initial pH and final pH, respectively.

2.5 Regeneration study

The spent TC's adsorption capability was investigated in regeneration study using three different washing solutions: distilled water, 0.1 mol L^{-1} HNO_3 and 0.1 mol L^{-1} NaOH. TC (1.0 g) was first treated with CV solutions (100 mg L^{-1}) using the optimised conditions obtained from the above experiments. The spent TC was then thoroughly washed with double distilled water before drying in an oven for 24 h at 85 °C. The dried TC-CV was then divided and agitated with the washing solutions mentioned for 1 h before washing thoroughly with double distilled water to get rid of the excess acid or base on the adsorbent. The samples were dried and then mixed with 100 mg L^{-1} dye solution. The adsorbed dye content was measured using UV-vis spectrophotometer. This is considered as one cycle. The treated adsorbent was again washed thoroughly with double distilled water to get rid of the remaining dye, acid or base on the adsorbent before drying in the oven for 24 h at 85 °C. The experiment was repeated for five consecutive cycles.

3. **Results and discussion**

3.1 Characterisations of adsorbent using FTIR and SEM

FTIR analysis is a very useful mean for the identification of the functional groups present on the sample's surface as different functional groups can absorb different levels of energy which is characteristic for each functional group. From Figure 1A, there are several functional groups being identified on TC, namely hydroxyl and/or amino (3384 cm^{-1}), methyl (2919 cm^{-1}) and carbonyl (1611 cm^{-1}). The band at 1245 cm^{-1} represents the C-O stretching band. After treatment with CV dye, the bands shifted to 3383, 2917, 1587 and 1244 cm^{-1} which might indicate the involvement of these functional groups in the dye-adsorbent interactions.

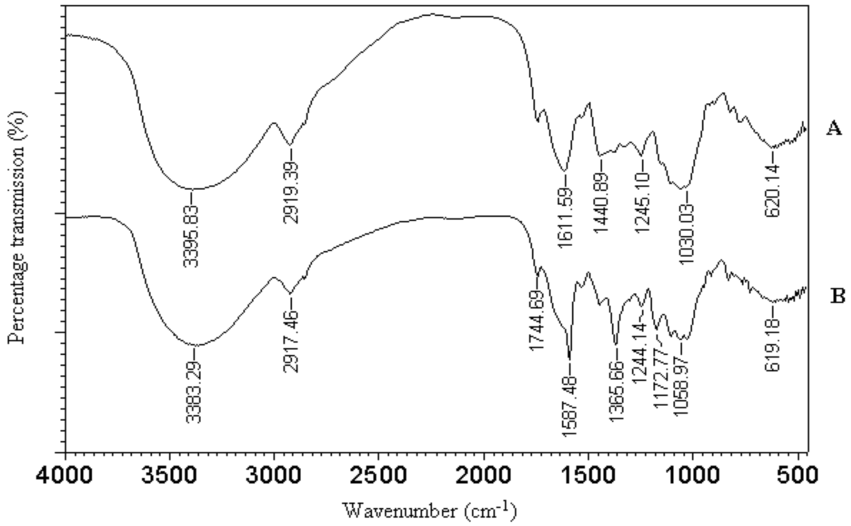

Figure 1: The FTIR spectra of A) TC and B) TC-CV

Scanning electron microscopy (SEM) is commonly used for the characterisation of the adsorbent's surface and provides valuable visual insights. As shown in Figure 2, the TC's surface appears to be irregular and rough in nature, thereby creating a large surface area for the adsorption of CV dye. This could account for the high q_m observed below in adsorption isotherm study.

3.2 Effect of dosage

The percentage removal of CV by using various amounts of TC was investigated and is shown in Figure 3. As can be seen, CV uptake increased from 0.01 g TC (70%) to 0.04 g TC (90%) due to the increasing amount of active sites available as the amount of TC increased. Beyond dosage of 0.04 g TC, the removal of CV became constant which might be due to the aggregation of TC caused by high dosage. The aggregation of the solid decreased the surface's active sites and thus, less dye molecules can be adsorbed. For this investigation, the 0.04 g of TC was chosen as the optimum dosage for further experiments.

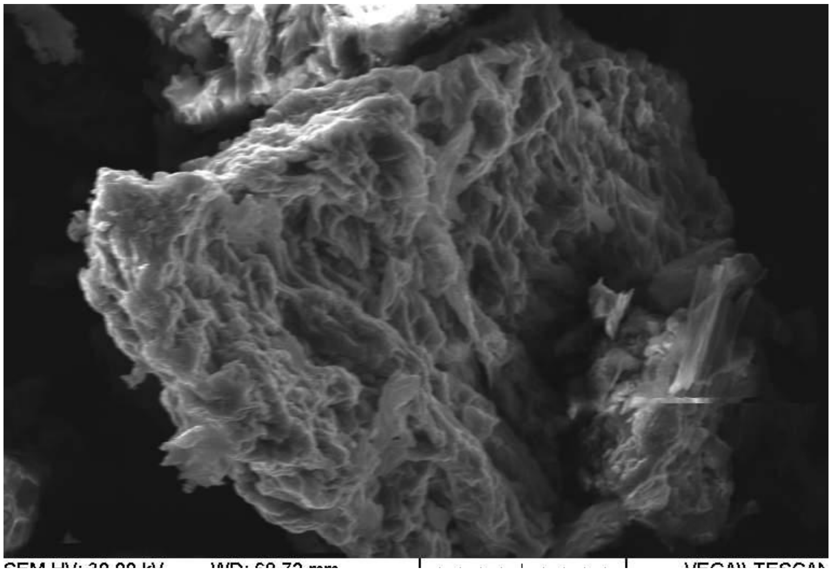

Figure 2: The SEM image of TC

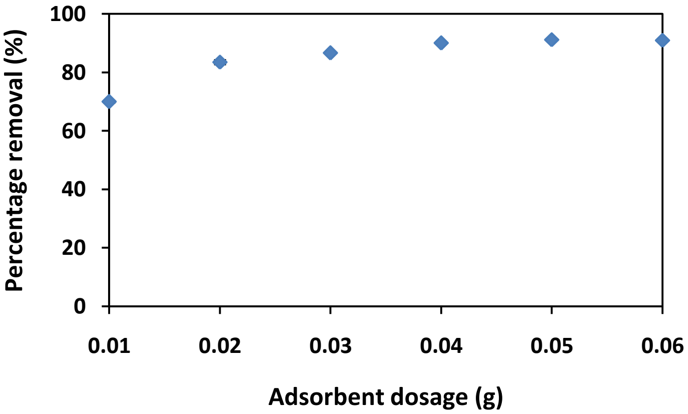

Figure 3: The effect of the amount of TC on the removal of CV from aqueous solution [dye volume = 20.0 mL; C_i = 100 mg L^{-1}; ambient pH & temperature; stirring rate = 250 rpm]

3.3 Effect of contact time and kinetics study

Contact time is investigated in the adsorption method in order to determine how fast the adsorption can equilibrate and for this purpose, the parameter is important for practical application. As observed in Figure 4A, the adsorption of 50 and 100 mg L^{-1} CV was very rapid and the q_e values were almost constant throughout the 4 h contact time. For 200 mg L^{-1} CV, there was a rapid increase in q_e from 5 min to 25 min and it became constant beyond this time. Rapid adsorption observed at the initial stage is due to the availability of vacant sites for the adsorption to take place. As these sites were gradually being filled, the rate decreased and finally reached a plateau at equilibrium. In order to ensure the adsorption completely equilibrates, 2 h contact time was chosen for further experiments.

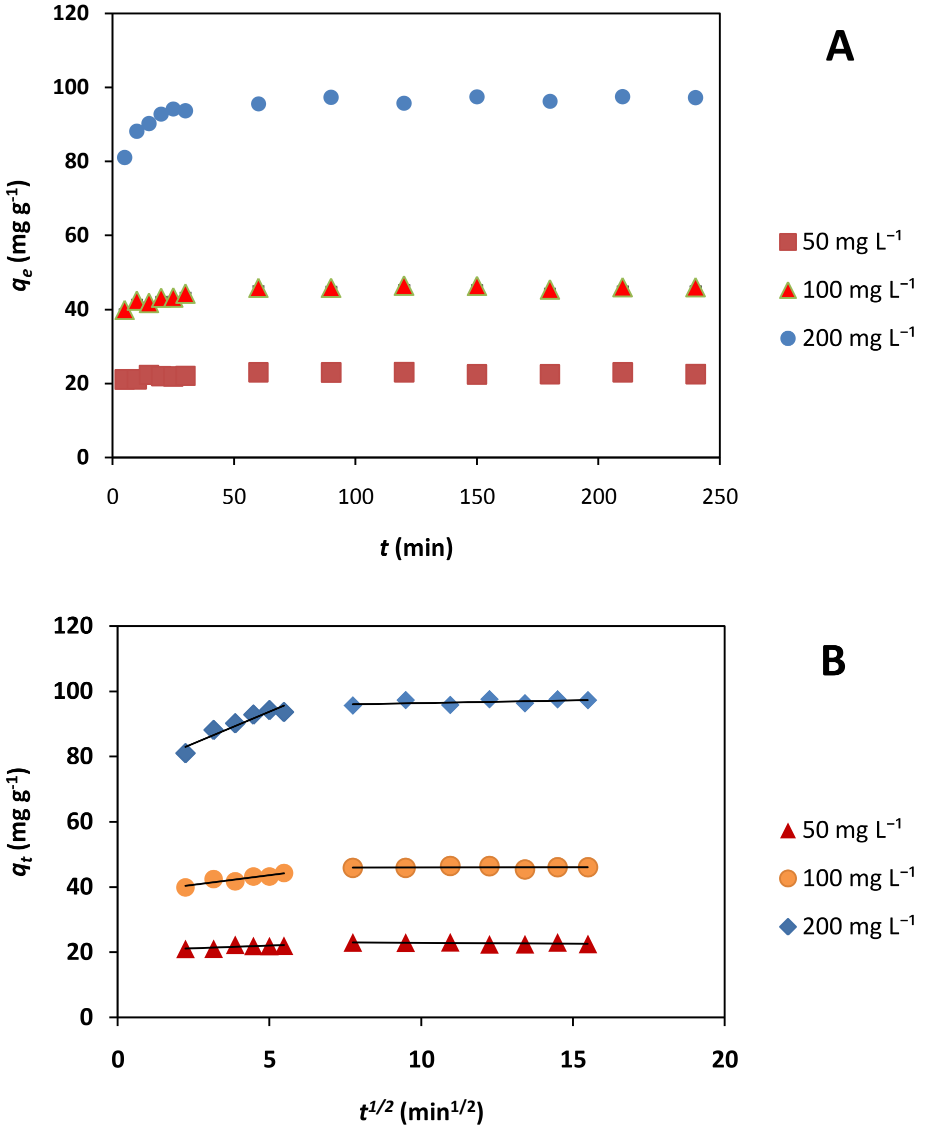

Figure 4: (A) Effect of contact time on the adsorption of 50, 100 and 200 mg L^{-1} CV by TC [dosage = 0.04 g; dye volume = 20.0 mL; ambient pH & temperature; stirring rate = 250 rpm] and (B) Weber-Morris plots for the adsorption of 50, 100 and 200 mg L^{-1} CV by TC

One of the important parameters for designing optimum operating conditions for adsorption process is the adsorption kinetics. The Lagergren 1st order [15], pseudo 2nd order [16], Weber-Morris intraparticle diffusion [17] and Boyd [18] models were used to describe the mechanism of the adsorption process. The linearised kinetics equations are shown below:

Lagergren 1st order model: $log\ (q_e - q_t) = log\ q_e - \frac{t}{2.303} k_1$ (3)

Pseudo 2nd order model: $\frac{t}{q_t} = \frac{1}{{q_e}^2 k_2} + \frac{t}{q_e}$ (4)

Weber-Morris intraparticle diffusion model: $q_t = k_3\, t^{1/2} + C$ (5)

Boyd model: $B_t = -0.4977 - ln\ (1 - F)$ (6)

where q_t is the amount of CV adsorbed per gram of TC (mg g^{-1}) at time t, t is the time shaken (min), k_1 is the 1st order rate constant (min^{-1}), k_2 is pseudo 2nd order rate constant (g mg^{-1} min^{-1}), k_3 is the intraparticle diffusion rate constant (mg g^{-1} min$^{-1/2}$), C is the intercept of the linear Weber-Morris plot which represents the thickness of the boundary layer, F is equivalent to q_t / q_e and B_t is the mathematical function of F.

Table 1 summarises the kinetics parameters for adsorption of 50, 100 and 200 mg L^{-1} CV by TC. The pseudo 2nd order model for all three CV concentrations has higher R^2 values than the Lagergren 1st order model indicating the former model to be a better fit to the experimental data than the latter. Furthermore, the calculated q_e ($q_{e,cal}$) values from pseudo 2nd order are in agreement with that of the experimental q_e ($q_{e,exp}$) values which further confirmed the suitability of the pseudo 2nd order in describing the experimental data. This suggests that electrostatic interaction and chemisorption whereby electron sharing and electron exchange between particles play major roles in the adsorption process [19].

Table 1: The kinetics parameters for the adsorption of CV by TC

C_i (mg L^{-1})	50	100	200
	Lagergren 1st order		
$q_{e,exp}$ (mg g^{-1})	22.54	46.04	97.23
$q_{e,cal}$ (mg g^{-1})	0.85	3.53	7.18
k_1 (min^{-1})	0.01	0.02	0.01
R^2	0.16	0.51	0.61
	Pseudo 2nd order		
$q_{e,exp}$ (mg g^{-1})	22.54	46.04	97.23
$q_{e,cal}$ (mg g^{-1})	22.73	46.25	97.64
k_2 (min^{-1})	0.13	0.02	0.01
R^2	1.00	1.00	1.00
	Weber-Morris intraparticle diffusion		
k_{3A} (mg g^{-1} min$^{-1/2}$)	0.33	1.17	3.92
C_A	20.40	37.70	74.18
k_{3B} (mg g^{-1} min$^{-1/2}$)	-0.05	0.004	0.17
C_B	23.43	45.93	94.73
	Boyd		
Slope	0.01	0.02	0.01
y-intercept	2.65	1.96	2.00
R^2	0.32	0.81	0.79

k_{3A} and k_{3B} are the intraparticle diffusion rate for first and second region in Figure 4B, respectively.

Since both the Lagergren 1st order and the pseudo 2nd order models do not give information on diffusion mechanism, both the Weber-Morris and Boyd diffusion models were employed instead. Generally, the Weber-Morris intraparticle diffusion involves three phases, namely fast initial external diffusion onto surface of adsorbent, intraparticle diffusion and slow final equilibrium stage. When the Weber-Morris linear plot passes through the origin, the intraparticle diffusion is considered as the rate limiting step of the adsorption process [17]. Figure 4B shows the Weber-Morris plots for 50, 100 and 200 mg L^{-1} CV which consist of two linear regions i.e. the fast initial adsorption phase was not observed. The intraparticle diffusion is presented by the first linear region while the second region (plateau) indicates the final equilibrium stage [20]. As both linear regions for all three CV concentrations do not pass through the origin as seen in Figure 4B and also indicated by the y-intercept (C_A and C_B) values shown in Table 1, the intraparticle diffusion is therefore not considered as the rate limiting step. The

Boyd model can be used as an indication of particle diffusion where the adsorption can occur within the pores if the linear plot passes through the origin. Otherwise, the adsorption occurs at the external surface (film diffusion) [21]. From Table 1, none of the intercept values (*C*) of the Boyd's plot passed through the origin and thus, the adsorption might be controlled by film diffusion.

3.4 Point of zero charge, effect of pH and effect of ionic strength

Point of zero charge (pH_{pzc}) is the determination of pH at which the surface has zero net charge. This is a useful tool to indicate the surface's charge as the pH is changed. At pH value higher than the pH_{pzc} of the adsorbent, the surface will be predominately negative in charge due to the deprotonation of the functional groups. On the other hand, lower pH value will cause the surface to be predominately positive in charge due to the protonation of the functional groups. In this experiment, TC was determined to have pH_{pzc} value of 4.20.

pH is an important parameter in adsorption studies as it can affect the adsorbents' surface charges and the ionisation of the dye molecules [22]. Figure 5A shows the effect of pH on the adsorption of CV by TC. The removal of CV was the lowest at pH 2 and increased from pH 4.38 (ambient pH) to 6.3, beyond which the removal was constant throughout the pH range studied. The dissociation constant (pKa) of CV is 9.4 [23].

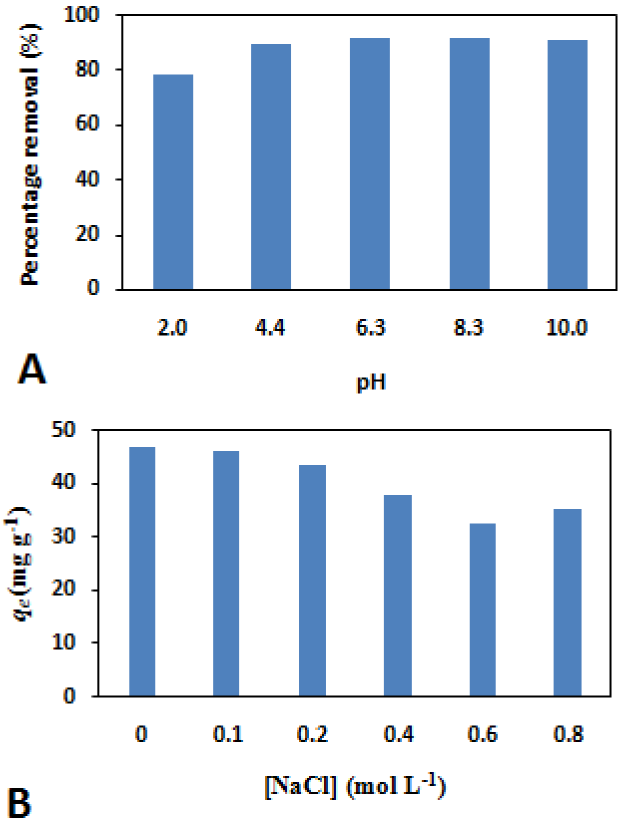

Figure 5: (A) Effect of pH on the adsorption of 100 mg L^{-1} CV by TC and (B) Effect of ionic strength on the adsorption of 100 mg L^{-1} CV by TC [dosage = 0.04 g; dye concentration = 100 mg L^{-1}; dye volume = 20.0 mL; ambient pH & temperature; stirring rate = 250 rpm]

Therefore at pH = 9.4, the ionic form and the neutral form of CV have equal concentrations according to the Henderson Hassalbalch equation, while at pH < pKa, the cationic form of CV predominates, and at pH > pKa, the corresponding anionic form of CV will predominate. At pH 2, where the pH < pKa, there is electrostatic repulsion between the TC's positively charged surface and cationic CV molecules due to the protonation of TC's functional groups such as amino group as discussed in the point of zero charge above. Also under strong acidic condition where the $[H^+]$ is expected to be high, there could also be competition between H^+ ions and the cationic CV for the adsorption sites. Hence the observed decrease in percentage removal of CV at pH 2. When the medium pH (pH 4.38 and beyond) is above pH_{PZC}, TC's surface net charge is predominantly negative which favours the interaction between the surface and the positively charged CV molecules. Even though there is an observed reduction in the removal, the adsorption of CV at pH 2 was not severely affected indicating that electrostatic interaction is not the main force and other interactions such as hydrophobic-hydrophobic interaction play a major role in the adsorption process [24]. The ambient pH of 100 mg L^{-1} CV solution was 4.38 where the removal of the dye at this pH is at 90% and thus, for this study, no pH adjustment was made.

Depending on the dyeing process, the dye wastewater will contain different salts with variety of amounts which leads to different water ionic strength. The presence of cations and anions from the salts in the water can either favour or interfere with the adsorption of adsorbates onto the adsorbents [25]. The q_e value in CV solution without salt was 47 mg g^{-1} which decreased to 35 mg g^{-1} in CV solution with 0.8 mol L^{-1} NaCl, as seen in Figure 5B. The decrease of the CV removal was due to the ionic suppression caused by the presence of Na^+ which competes with CV molecules for TC's active sites. As the adsorption of CV onto TC was not dependent on electrostatic interaction as discussed above, the adsorption process was not severely affected by the presence of the salt. This can be seen as an advantage of using TC as an adsorbent in treatment of wastewater with high ionic strength.

3.5 Effect of temperature and thermodynamics study

The effect of temperature on the adsorption of CV onto TC is presented in Table 2 whereby the q_e values increased as the temperature increases. As the temperature increased, movement of dye molecules also increased, thereby resulting in more adsorbent-adsorbate interactions [26] and also increasing the penetration of dye molecules into the adsorbent [27]. Gibbs free energy ($\Delta G°$), enthalpy ($\Delta H°$) and entropy ($\Delta S°$) were obtained from the Van't Hoff equation as shown below,

$$\Delta G^0 = -RTlnK \qquad (7)$$

$$K = \frac{C_s}{C_e} \qquad (8)$$

$$\Delta G^0 = \Delta H^0 - T\Delta S^0 \qquad (9)$$

Inserting eq (7) into eq (9):

$$\ln K = \frac{\Delta S^o}{R} - \frac{\Delta H^o}{RT} \qquad (10)$$

where C_S is the amount of CV adsorbed on TC at equilibrium (mg L^{-1}), R is the gas constant (J K^{-1} mol^{-1}) and T is the absolute temperature (K).

As seen in Table 2, the $\Delta G°$ values became more negative with the increase of temperature indicating the adsorption process is feasible and more favourable at higher temperature. The positive $\Delta H°$ value showed that the adsorption process was endothermic in nature while positive $\Delta S°$ value indicated an increase in randomness in the system and could be a result of "solvent-replacement" phenomenon, where the water molecules on the surface were replaced by the dye molecules and thus, increase in randomness [28]. It is noted that, even though the data showed an increase in the spontaneity of the system at higher temperature, the values of $\Delta G°$ and q_e did not differ by much i.e. from -4.0 to -5.2 kJ mol^{-1}. Thus, it can be said that the adsorption of CV by TC is not significantly affected by temperature.

Table 2: The q_e values and thermodynamics parameters at various temperatures

T (K)	$\Delta G°$ (kJ mol^{-1})	$\Delta H°$ (kJ mol^{-1})	$\Delta S°$ (J mol^{-1} K^{-1})	q_e (mg g^{-1})
298	-4.0	5.1	30.5	67.6
313	-4.2			66.5
323	-4.8			70.4
333	-5.0			69.9
343	-5.2			70.2

3.6 Effect of dye concentration and adsorption isotherm modelling

The removal of CV by TC increased from 11 mg g^{-1} (C_i = 20 mg L^{-1}) to 180 mg g^{-1} (C_i = 500 mg L^{-1}), as shown in Figure 6. The increase is caused by the driving force provided from concentration gradient in order to overcome the mass transfer resistance of the dye molecules from the bulk solution to the adsorbent's surface [29].

The Langmuir [30], Freundlich [31] and Tempkin [32] isotherm models, whose equations are shown in Table 3, were used in the prediction of the adsorption process of CV onto TC. The Langmuir isotherm model assumes that the adsorption occurs only as one layer of adsorbate covering the surface i.e. monolayer adsorption [30]. The separation factor (R_L) is a dimensionless constant which can be calculated from the Langmuir model and is given by the following equation,

$$R_L = \frac{1}{(1+bC_o)} \qquad (11)$$

The value of R_L determines if the Langmuir isotherm model is unfavourable ($R_L > 1$), linear ($R_L = 1$), favourable ($0 < R_L < 1$), or irreversible ($R_L = 0$) [33].

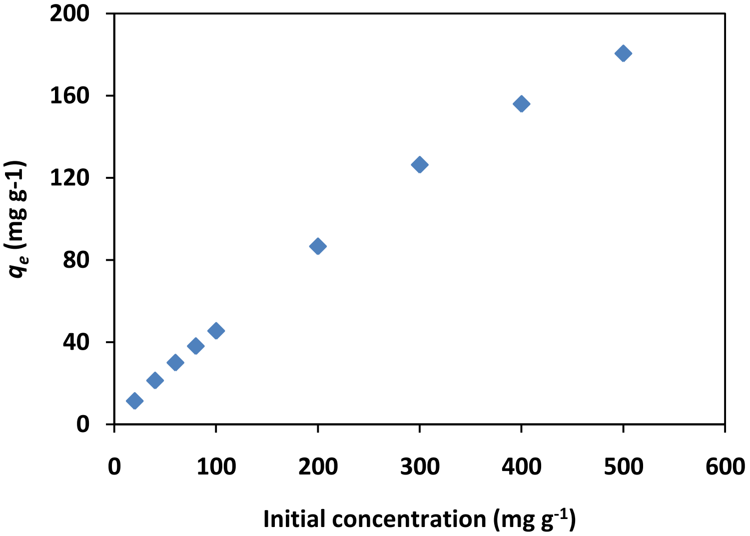

Figure 6: The effect of dye concentration on the adsorption of CV onto TC [dosage = 0.04 g; dye concentration = 20 – 500 mg L^{-1}; dye volume = 20.0 mL; ambient pH & temperature; stirring rate = 250 rpm].

The Freundlich isotherm model assumes the adsorbent's surface can have more than one layer of adsorbate covering it and is applicable for adsorption on heterogeneous surfaces [31]. The Tempkin isotherm model assumes coverage leads to linear decrease of heat energy which differs from the Freundlich model [32].

Error function analysis namely the chi-square test (χ^2) is used to compare the suitability of each isotherm model in describing the experimental data whereby smaller χ^2 values indicate the better curve fitting [34].

$$\chi^2 : \sum_{i=1}^{n} \frac{(q_{e,meas} - q_{e,calc})^2}{q_{e,meas}} \qquad (12)$$

where $q_{e,meas}$ is the adsorption capacity obtained experimentally while $q_{e,calc}$ is the calculated/predicted adsorption capacity and n is the number of data in the experiment.

Table 4 shows the calculated Langmuir, Freundlich and Tempkin isotherm models' parameters. Comparing between these three models, it can be seen that all of them have high correlation coefficient (R^2) values of >0.95 whereby the Langmuir model has the highest R^2 value followed by Freundlich and Tempkin. This indicates that the Langmuir model can describe the experimental data the best. The Langmuir model's χ^2 value is the smallest amongst the three models which further support the suitability of the Langmuir model with the experimental data. This shows that CV was adsorbed onto TC forming a monolayer. The values of R_L and n_F both indicate the favourability of the adsorption process. The performance of TC in removing CV from aqueous solution is superior compared to many adsorbents, as summarised in Table 5. This shows the potential of TC to be used as an adsorbent.

Table 3: The Langmuir, Freundlich and Tempkin isotherm equations

Isotherm model	Non-linear equation	Linearised equation
Langmuir	$q_e = \frac{q_m b C_e}{1 + bC_e}$	$\frac{C_e}{q_e} = \frac{1}{b\, q_m} + \frac{C_e}{q_m}$
Freundlich	$q_e = K_F C_e{}^{1/n_F}$	$ln q_e = \frac{1}{n_F} lnC_e + lnK_F$
Tempkin	$q_e = \frac{RT}{b_t} \ln K_T C_e$	$q_e = \frac{RT}{b_T} \ln K_T + \frac{RT}{b_T} \ln C_e$

where q_m is the maximum monolayer adsorption capacity of the adsorbent (mg g^{-1}), b is the Langmuir adsorption constant (L mg^{-1}), K_F [mg g^{-1}(L $mg^{-1})^{1/n}$] is the adsorption capacity of the adsorbent, n_F represents the Freundlich constant, K_T is the equilibrium binding constant and b_T is the Tempkin constant (kJ mol^{-1}).

Table 4: The isotherm models' parameters and χ^2 values

Langmuir		Freundlich		Tempkin	
q_m (mg g^{-1})	217.031	K_F [mg g^{-1}(L $mg^{-1})^{1/n}$]	11.194	bt (kJ mol^{-1})	0.063
b (L mg^{-1})	0.032	n_F	1.669	K_T	0.528
R_L	0.060				
R^2	0.987	R^2	0.981	R^2	0.952
χ^2	4.950	χ^2	9.570	χ^2	51.120

Table 5: The comparison between various adsorbents' q_m values

Adsorbents	q_m (mg g^{-1})	Reference
TC	217.00	This work
Tarap leaf	50.50	[35]
Tarap peel	118.00	[36]
Jackfruit leaf powder	43.40	[37]
Treated ginger waste	64.93	[38]
Tomato plant root	94.34	[39]
Peat	108.00	[9]
Yeast treated peat	17.95	[10]
Breadfruit	145.80	[4]

3.7 Regeneration study

After the adsorbate is adsorbed onto the adsorbent, the used adsorbent itself can be treated as a hazardous waste which can cause environmental problems if it is not properly disposed [40]. Regeneration of this used adsorbent can be performed as an alternative as it can also minimise the cost for waste disposal. The used adsorbents can be subjected to chemical treatments such as treatment with acid, base and chelating agents or through physical means by thermal heating using furnace or microwave in order to regenerate their adsorption capabilities [41, 42]. As shown in Figure 7, it can be seen that all the washing solutions managed to regenerate TC's adsorption capability even after five cycles. The effectiveness of using these three washing solutions, particularly distilled water proved to be very advantageous as it is being extremely easy, cheap and needs almost no machinery to perform.

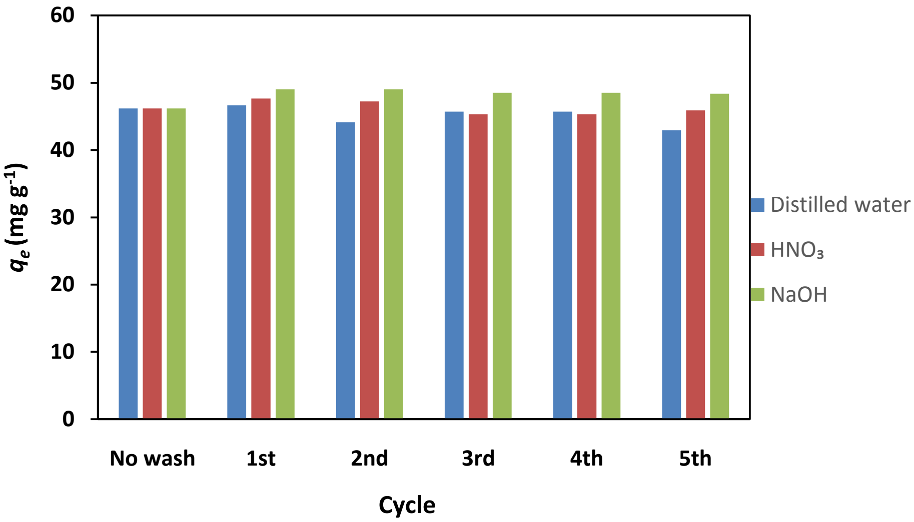

Figure 7: The regeneration of spent TC over five cycles using distilled water, NaOH and HNO_3

Conclusions

The removal of CV from aqueous solution by TC has high q_m value when compared to many reported adsorbents. Fast kinetics coupled with TC's ability to operate well in a range of temperature and pH as well as can be regenerated using water, base and acid makes TC to be a reliable adsorbent to be used. Adsorption is thermodynamically feasible and endothermic in nature. It follows the pseudo 2nd order model which indicates that chemisorption may be involved in the adsorption process. All these factors show the potential of TC to be used as a cheap and effective alternative adsorption material.

Acknowledgments-The authors are pleased to acknowledge the Government of Brunei Darussalam and Universiti Brunei Darussalam (UBD) for their offer of Graduate Research Studies scholarship.

References

1. Gupta V.K., Suhas. *J. Environ. Manag*. 90 (2009) 2313.
2. Nelson C.R., Hites R.A., *Environ. Sci. Technol.* 14 (1980) 1147.
3. Suresh S., *Current Environ. Eng.* 1 (2016) 162.
4. Lim L.B.L., Priyantha N., Mansor N.M., *Environ. Earth Sci*. 73 (2015) 3239.
5. Kooh M.R.R., Dahri M.K., Lim L.B., Lim L.H., *Arab. J. Sci. Eng.* 41 (2016) 2453.
6. Kooh M.R.R., Lim L.B.L., Lim L.H., Dahri M.K., *Environ. Monitor. Assess.* 188 (2016) 108.
7. Kooh M.R.R., Lim L.L., Dahri M.K., Lim L.H., Sarath Bandara J.M.R., *Waste Biomass Valor.* 6 (2015) 547.
8. Dahri M.K., Kooh M.R.R., Lim L.B.L., *J. Environ. Chem. Eng.* 2 (2014) 1434.
9. Chieng H.I., Lim L.B.L., Priyantha N., Tennakoon D.T.B., *Int. J. Earth Sci. Eng.* 6 (2013) 791.
10. Zehra T., Priyantha N., Lim L.B.L., *Environ. Earth. Sci.* 75 (2016) 1.
11. Chieng H.I., Lim L.B.L., Priyantha N., *Desalin. Water Treat.* 55 (2015) 664.
12. Lim L.B.L., Priyantha N., Tennakoon D.T.B., Dahri M.K., *Environ. Sci. Pollut. Res. Int.* 19 (2012) 3250.
13. Kooh M.R.R., Dahri M.K., Lim L.B.L., *Appl. Water Sci.* (2016) 1.
14. Sabnis R.W. Handbook of biological dyes and stains: synthesis and industrial applications. Hoboken, New Jersey: John Wiley & Sons; 2010.
15. Lagergren S., *K. Svenska. Vetenskapsakad. Handl.* 24 (1898) 1.
16. Ho Y.S., McKay G., *Process Biochem.* 34 (1999) 451.
17. Weber W., Morris J., *J. Sanit. Eng. Div.* 89 (1963) 31.

18. Boyd G.E., Adamson A.W., Myers L.S., *J. Am. Chem. Soc.* 69 (1947) 2836.
19. Li G., Zhang D., Li Q., Chen G., *Environ. Earth Sci.* 72 (2014) 4237.
20. Gad H.M.H., El-Sayed A.A., *J. Hazard. Mater.* 168 (2009) 1070.
21. Tavlieva M.P., Genieva S.D., Georgieva V.G., Vlaev L.T., *J. Colloid Interf. Sci.* 409 (2013) 112.
22. Saha P., Chowdhury S., Gupta S., Kumar I., *Chem. Eng. J.* 165 (2010) 874.
23. Sabnis R.W. Handbook of Acid-Base Indicators: CRC Press; 2007.
24. Hu Y., Guo T., Ye X., Li Q., Guo M., Liu H., Wu Z., *Chem. Eng. J.* 228 (2013) 392.
25. Aguedach A., Brosillon S., Morvan J., Lhadi E.K., *J. Hazard. Mater.* 150 (2008) 250.
26. Senthilkumaar S., Kalaamani P., Subburaam C.V., *J. Hazard. Mater.* 136 (2006) 800.
27. Al-Degs Y.S., El-Barghouthi M.I., El-Sheikh A.H., Walker G.M., *Dyes Pigments*. 77 (2008) 16.
28. Ruixia W., Jinlong C., Lianlong C., Zheng-hao F., Ai-min L., Quanxing Z., *React. Func. Pol.* 59 (2004) 243.
29. Chowdhury S., Das P., *Environ. Prog. Sust. Energy*. 31 (2012) 415.
30. Langmuir I., *J. Am. Chem. Soc.* 38 (1916) 2221.
31. Freundlich H.M.F., *J. Phys. Chem.* 57 (1906) 385.
32. Tempkin M.I., Pyzhev V., *Acta Physiochim. USSR*. 12 (1940) 327.
33. McKay G., Blair H.S., Gardner J.R., *J. Appl. Poly. Sci.* 27 (1982) 3043.
34. Tsai S.C., Juang K.W., *J. Radioanal. Nucl. Chem.* 243 (2000) 741.
35. Lim L.B.L., Priyantha N., Cheng H.H., Zaidi N.A.H.M., *J. Environ. Biotechnol. Res.* 4 (2016) 32.
36. Lim L.B.L., Priyantha N., Zehra T., Then C.W., Chan C.M., *Desalin. Water Treat.* 57 (2016) 10246.
37. Saha P.D., Chakraborty S., Chowdhury S., *Colloid. Surf. B: Biointerf.* 92 (2012) 262.
38. Kumar R., Ahmad R., *Desalination*. 265 (2011) 112.
39. Kannan C., Buvaneswari N., Palvannan T., *Desalination*. 249 (2009) 1132.
40. Qu G.-Z., Li J., Wu Y., Li G.-F., Li D., *Chem. Eng. J.* 146 (2009) 168.
41. Polaert I., Estel L., Huyghe R., Thomas M., *Chem. Eng. J.* 162 (2010) 941.
42. Guo D., Shi Q., He B., Yuan X., *J. Hazard. Mater.* 186 (2011) 1788.

(2017) ; http://www.jmaterenvironsci.com